Integrated Guidance and Control for Homing Missiles with Terminal Angular Constraint in Three Dimension Space

Shichao Ma
Northwestern Polytechnical University
Xi'an, P.R.China
shichao_ma@mail.nwpu.edu.cn

Aijun Li
Northwestern Polytechnical University
Xi'an, P.R.China
liaijun@nwpu.edu.cn

Zhigang Wang
Northwestern Polytechnical University
Xi'an, P.R.China
wang_zhigang@mail.nwpu.edu.cn

***Abstract*—A three dimension integrated guidance and control (3D-IGC) system for homing missiles with terminal angle constraint is designed. Firstly, a nonlinear mathematical model of the homing missile is established. In order to deal with the problem of multiple states regulation of such a nonlinear system, an adaptive multiple sliding surface control methodology is deduced. The frame of 3D-IGC law is accomplished by associating with the backstepping method. The digital simulation results verify that the proposed control law can both satisfy the accuracy of target interception and the constrained conditions of terminal angular. Moreover, it shows strong robustness against parameter uncertainties.**

Keywords—Adaptive multiple sliding surface control, backstepping, 3D-IGC, terminal angular constraint.

I. INTRODUCTION

The conventional design scheme of the homing missile guidance and control system is to design each subsystem personally and then put them into one framework, which basically guaranteed the requirements of accurately intercepting targets [1]. However, it is proposed that this design method may not fully take advantage of the synergy relationships between the two interacting systems [2]. What's more, for the purpose of satisfying the expected overall system performance, alterations are usually necessary to each subsystem which leads to huge workloads and high costs. To deal with such a problem, the integrated guidance and control (IGC) design method was first proposed by Williams [3].

The IGC is proposed to generate the fin deflection commands according to the states of the missile and the target states associated to the missile to drive the missile to intercept the target [4], which means using the full nonlinear dynamics in a single unified framework. Therefore, comparing with the traditional design method, the IGC is generally considered to be capable of developing the inherent coupling that consists between the guidance and control system, which can help to achieve optimal performance of the overall system.

Since the concept of IGC was presented, different effective control methods have been proposed successively. Approach like sliding mode control [5], small-gain theorem [6] and dynamic inversion [7] have been used in the design of the IGC framework.

The researches above mainly focus on the IGC without the constraint of terminal angular. In this article, aiming at a 3D-IGC system with terminal angle constraint model for homing missile, an adaptive multiple sliding surface control approach combined with the backstepping method is developed. The mathematical derivation process of the stability analysis of the proposed controller is also given via the Lyapunov stability theory. The digital simulation results have verified that the designed control law can satisfy both the precision of target interception and the desired terminal constraint angles.

II. MATHEMATICAL MODEL DESCRIPTION

In this part, the 3D-IGC mathematical model of a homing missile is firstly established.

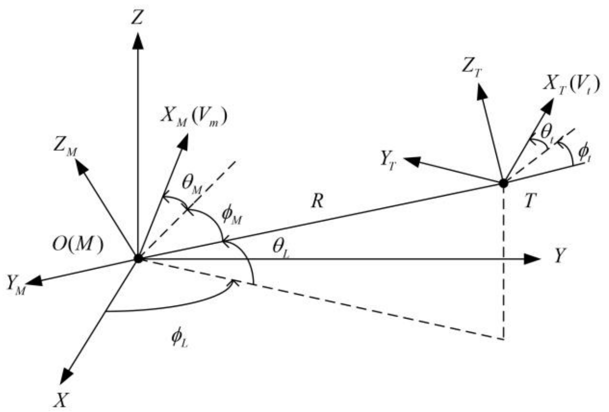

Fig. 1 Geometry in a 3-D space.

Where $O-XYZ$ represents the inertial coordinate system, $M-X_MY_MZ_M(T-X_TY_TZ_T)$ represent the velocity coordinate system of the missile and the target, R is the missile-target range, $V_m(V_t)$ are the velocity of the missile and the target, $\theta_m,\phi_m(\theta_t,\phi_t)$ are the angular of the velocity of the missile (target) relative to the line-of-sight (LOS) coordinate system, θ_L,ϕ_L the elevation angle and the azimuth angle of the LOS.

Firstly, the relative kinematics equations of the missile intercepting mobile targets are given:

978-1-7281-6590-5/20/$31.00 ©2020 IEEE Dalian, China
March 20-22, 2020

$$\begin{cases} \ddot{R} - R\dot{\theta}_L^2 - R\dot{\phi}_L^2 \cos^2 \theta_L = a_{tR} - a_{mR} \\ R\ddot{\theta}_L + 2\dot{R}\dot{\theta}_L + R\dot{\phi}_L^2 \sin\theta_L \cos\theta_L = a_{t\theta} - a_{m\theta} \\ -R\ddot{\phi}_L \cos\theta_L - 2\dot{R}\dot{\phi}_L \cos\theta_L + 2R\dot{\theta}_L\dot{\phi}_L \sin\theta_L = a_{t\phi} - a_{m\phi} \end{cases} \quad (1)$$

Where a_{mR} $a_{m\theta}$ $a_{m\phi}$ and a_{tR} $a_{t\theta}$ $a_{t\phi}$ respectively represent the acceleration of the missile and the target in the LOS coordinate system. θ is the flight path angle.

Then consider the relationship between missile acceleration and aerodynamic forces. The aerodynamic forces of the homing missile in the velocity coordinate system are shown as:

$$\begin{cases} a_{mz} = \dfrac{Z}{m} \\ a_{my} = \dfrac{Y}{m} \\ Y = qS(c_y^\alpha \alpha + c_y^\beta \beta + c_y^{\delta_z} \delta_z) \\ Z = qS(c_z^\alpha \alpha + c_z^\beta \beta + c_z^{\delta_y} \delta_y) \end{cases} \quad (2)$$

Where m is the missile mass, a_{mz} and a_{my} are the missile acceleration in the body coordinate system, $q = \frac{1}{2}\rho V_m^2$ is the dynamic pressure, S is the reference area, ρ is the air mass density. α , β are the angle of attack and sideslip, δ_y , δ_z are the deflection of rudder and elevator. c_y^α , c_y^β and $c_y^{\delta_z}$ are some partial derivatives of lift force coefficient. c_z^α , c_z^β and $c_z^{\delta_y}$ are some partial derivatives of yawing force coefficient.

By some coordinate transformation, the dynamics equation of the LOS angles can be summarized as:

$$\begin{cases} \ddot{\theta}_L = -\dot{\phi}_L^2 \sin\theta_L \cos\theta_L - \dfrac{2\dot{R}\dot{\theta}_L}{R} - M_1 Y \cos(\gamma_V) \\ \quad -\dfrac{\sin\theta_L \sin(\phi_L - \varphi_V)}{mR}(Y\cos(\gamma_V) + Z\sin(\gamma_V)) \\ \quad +M_1(mg\cos\theta + Z\sin(\gamma_V)) + d_{\theta L} \\ \ddot{\phi}_L = -\dfrac{2\dot{R}\dot{\phi}_L}{R} + 2\dot{\theta}_L\dot{\phi}_L \tan\theta_L - M_2 Y\cos(\gamma_V) \\ \quad +\dfrac{\cos(\phi_L - \varphi_V)}{mR\cos\theta_L}(Y\cos(\gamma_V) + Z\sin(\gamma_V)) \\ \quad +M_2(mg\cos\theta + Z\sin(\gamma_V)) + d_{\phi L} \end{cases} \quad (3)$$

Where $M_1 = \dfrac{\cos\theta\cos\theta_L + \sin\theta\sin\theta_L\cos(\phi_L - \varphi_v)}{mR}$, $M_2 = \dfrac{\sin\theta\cos(\phi_L - \varphi_v)}{mR\cos\theta_L}$, φ_v is the ballistic angle, γ_V the roll angle, $d_{\theta L}$ and $d_{\phi L}$ the approximation errors of θ_L and ϕ_L .

The kinematics equations of the trajectory inclination angle and ballistic angle are shown as:

$$\begin{cases} \dot{\theta} = \dfrac{Y\cos\gamma_V - Z\sin\gamma_V - mg\cos\theta}{mV_m} \\ \dot{\varphi}_v = \dfrac{-Y\sin\gamma_V - Z\cos\gamma_V}{mV_m\cos\theta} \end{cases} \quad (4)$$

The kinematic and dynamic equations of missile rotating around the center of mass in the 3D space are given:

$$\begin{cases} \dot{\alpha} = -\omega_x \tan\beta\cos\alpha + \omega_y \tan\beta\sin\alpha + \omega_z \\ \quad -\dfrac{Y}{mV_m\cos\beta} + \dfrac{g\cos\theta\cos\gamma_V}{V_m\cos\beta} \\ \dot{\beta} = \omega_x \sin\alpha + \omega_y \cos\alpha + \dfrac{Z + mg\cos\theta\sin\gamma_V}{mV_m} \\ \dot{\gamma}_V = \cos\alpha\sec\beta\omega_x - \sin\alpha\sec\beta\omega_y \\ \quad +\dfrac{Y(\tan\theta\sin\gamma_V + \tan\beta) + Z\tan\theta\cos\gamma_V}{mV_m} \\ \quad -\dfrac{\cos\theta\cos\gamma_V\tan\beta}{V_m} g \end{cases} \quad (5)$$

$$\begin{cases} \dot{\omega}_x = \dfrac{J_y - J_z}{J_x}\omega_z\omega_y + \dfrac{M_x}{J_x} \\ \dot{\omega}_y = \dfrac{J_z - J_x}{J_y}\omega_x\omega_z + \dfrac{M_y}{J_y} \\ \dot{\omega}_z = \dfrac{J_x - J_y}{J_z}\omega_y\omega_x + \dfrac{M_z}{J_z} \end{cases} \quad (6)$$

$$\begin{cases} M_x = qSL(m_x^\alpha \alpha + m_x^\beta \beta + m_x^{\delta_x} \delta_x) \\ M_y = qSL(m_y^\beta \beta + m_y^{\delta_y} \delta_y) \\ M_z = qSL(m_z^\alpha \alpha + m_z^{\delta_z} \delta_z) \end{cases} \quad (7)$$

Where L is the reference length. m_x^α , m_x^β and $m_x^{\delta_x}$ are some partial derivatives of rolling moment coefficient. m_y^β , $m_y^{\delta_y}$ are some partial derivatives of yawing moment coefficient. m_z^α and $m_z^{\delta_z}$ are some partial derivatives of pitching moment coefficient. J_x , J_y and J_z are the inertia coefficient in the roll, yaw and pitch channel. ω_x 、 ω_y and ω_z are the roll, yaw and pitch angle rates in the body axis. $g = 9.8m/s^2$ is the gravity acceleration.

Assume that θ_{Lf} and ϕ_{Lf} are the desired LOS angle. As is stated in [8], we can learn that the desired terminal angle θ_L and ϕ_L about equal to the desired terminal LOS angle θ_{Lf} and ϕ_{Lf} .

Based on the above analysis, the 3D-IGC mathematical model of the homing missile can be summarized as:

$$\begin{cases} \dot{x}_0 = x_1 \\ \dot{x}_1 = f_1 + b_1\bar{x}_2 + d_1 \\ \dot{x}_2 = f_2 + b_2x_3 + d_2 \\ \dot{x}_3 = f_3 + b_3u + d_3 \end{cases} \quad (8)$$

Where $x_0 = \begin{bmatrix} \theta_L - \theta_{Lf} \\ \phi_L - \phi_{Lf} \end{bmatrix}$, $x_1 = \begin{bmatrix} \dot{\theta}_L \\ \dot{\phi}_L \end{bmatrix}$, $x_2 = \begin{bmatrix} \alpha \\ \beta \\ \gamma_v \end{bmatrix}$, $x_3 = \begin{bmatrix} \omega_x \\ \omega_y \\ \omega_z \end{bmatrix}$, $u = \begin{bmatrix} \delta_x \\ \delta_y \\ \delta_z \end{bmatrix}$. $d_i(i=1,2,3)$ represent the approximate errors of the system. The specific form of the system can be shown as:

$$d_1 = \begin{bmatrix} d_{11} \\ d_{12} \end{bmatrix}, d_2 = \begin{bmatrix} d_{21} \\ d_{22} \\ d_{23} \end{bmatrix}, d_3 = \begin{bmatrix} d_{31} \\ d_{32} \\ d_{33} \end{bmatrix},$$

$$b_1 = \begin{bmatrix} -M_1 qSc_y^{\alpha} & -\dfrac{qSc_z^{\beta} \sin\theta_L \sin(\phi_L - \varphi_V)}{mR} \\ -M_2 qSc_y^{\alpha} & \dfrac{qSc_z^{\beta} \cos(\phi_L - \varphi_V)}{mR\cos\theta_L} \end{bmatrix},$$

$$b_2 = \begin{bmatrix} -\tan\beta\cos\alpha & \tan\beta\sin\alpha & 1 \\ \sin\alpha & \cos\alpha & 0 \\ \cos\alpha\sec\beta & -\sin\alpha\sec\beta & 0 \end{bmatrix},$$

$$b_3 = \begin{bmatrix} \dfrac{qSLm_x^{\delta_x}}{J_x} & 0 & 0 \\ 0 & \dfrac{qSLm_y^{\delta_y}}{J_y} & 0 \\ 0 & 0 & \dfrac{qSLm_z^{\delta_z}}{J_z} \end{bmatrix}$$

$$f_1 = \begin{bmatrix} -\dfrac{2\dot{R}}{R}\dot{\theta}_L - \dot{\phi}_L^2 \sin\theta_L \cos\theta_L + M_1 mg\cos\theta \\ -\dfrac{2\dot{R}}{R}\dot{\phi}_L + 2\dot{\theta}_L\dot{\phi}_L \tan\theta_L + M_2 mg\cos\theta \end{bmatrix}$$

$$f_2 = \begin{bmatrix} -\dfrac{qSY_y}{mV\cos\beta} + \dfrac{g}{V\cos\beta}\cos\gamma \\ -\dfrac{qSZ_z}{mV} + \dfrac{g}{V}\cos\theta\sin\gamma \\ -\dfrac{F_{YZ}}{mV} - \dfrac{g}{V}\cos\theta\cos\gamma\tan\beta \end{bmatrix}$$

$$f_3 = \begin{bmatrix} \dfrac{J_y - J_z}{J_x}\omega_z\omega_y + \dfrac{qSL(m_x^{\alpha}\alpha + m_x^{\beta}\beta)}{J_x} \\ \dfrac{J_z - J_x}{J_y}\omega_x\omega_z + \dfrac{qSLm_y^{\beta}\beta}{J_y} \\ \dfrac{J_x - J_y}{J_z}\omega_y\omega_x + \dfrac{qSLm_z^{\alpha}\alpha}{J_z} \end{bmatrix}$$

$$Y_y = c_y^{\alpha}\alpha + c_y^{\beta}\beta$$

$$Z_z = c_z^{\alpha}\alpha + c_z^{\beta}\beta,$$

$$F_{YZ} = qS(Y_y(\tan\theta\sin\gamma + \tan\beta) + Z_z\tan\theta\cos\gamma)$$

The object of the next chapter is to devise a good performance control law for the proposed 3D-IGC system, which can simultaneously guarantee a reasonable miss distance and desired terminal LOS angles.

III. CONTROLLER DESIGN AND PROOF OF STABILITY

In this part, an adaptive multiple sliding surface control approach combined with backstepping method is devised for the 3D-IGC model (8).

A. Control algorithm

Assumption 1: k_{ij} are some unknown positive constants which we have $|d_{ij}| \le k_{ij}$.

For such a nonlinear model of 3D-IGC system (8), the backstepping approach has been widely used in the process of control design. Nevertheless, the traditional backstepping method encounters the problem of "explosion of complexity" caused by the repeated derivative calculations of the deduced virtual control vectors.

In order to deal with such a problem, a series of first-order filters are utilized. Meanwhile, an adaptive multiple dynamic surface control law is adopted to estimate the upper bound of the model uncertainties $d_i(i=1,2,3)$.

The controller is given as follow:

$$\begin{cases} S_1 = \begin{bmatrix} S_{11} & S_{12} \end{bmatrix}^T = x_1 + cx_0 \\ \tilde{x}_{2d} = -b_1^{-1}(f_1 + \tau_1 S_1 + P_1\hat{k}_1 + cx_1) \\ T_1\dot{x}_{2c} + x_{2c} = \tilde{x}_{2d} \\ S_2 = \begin{bmatrix} S_{21} & S_{22} & S_{23} \end{bmatrix}^T = x_2 - \begin{bmatrix} x_{2c} & 0 \end{bmatrix}^T \\ x_{3d} = -b_2^{-1}(f_2 + \tau_2 S_2 + P_2\hat{k}_2 - \begin{bmatrix} \dot{x}_{2c} & 0 \end{bmatrix}^T) \\ T_2\dot{x}_{3c} + x_{3c} = x_{3d} \\ S_3 = \begin{bmatrix} S_{31} & S_{32} & S_{33} \end{bmatrix}^T = x_3 - x_{3c} \\ u = -b_3^{-1}(f_3 + \tau_3 S_3 + P_3\hat{k}_3 - \dot{x}_{3c}) \end{cases} \tag{9}$$

Where S_1 , S_2 , S_3 are the sliding dynamic surface vectors; $\tau_1 = diag(\tau_{11}, \tau_{12})$, (τ_2 , τ_3 have the same form) are the dynamic surface gain matrices. c is a positive constant.

The design process of the control law involves three steps. $\tilde{x}_{2d}$ and $\tilde{x}_{3d}$ represent the virtual control vectors deduced from the first two steps. x_{2c} and x_{3c} represent the actual inputs of the after two steps, which can be acquired by letting $\tilde{x}_{2d}$ and $\tilde{x}_{3d}$ separately transit through a series of first-order filters,. T_1 and T_2 are the filter time positive constant diagonal matrices. $P_i = diag(sign(S_{ij}))$.

$\hat{k}_i$ is the estimation of the model uncertainties d_i, which are governed by the following adaptive law:

$$\dot{\hat{k}}_i = r_i\zeta_i \tag{10}$$

Where $r_i \geq 1$ is the design parameter, $\zeta_i = |S_i|$.

B. Proof of Stability

Theorem 1: The nonlinear system described by (8) is stable by using controller (9). Specifically, the states are all bounded and the outputs asymptotically converge to zero under the Assumption 1.

The mathematical derivation of theorem proving is given.

Mathematical proof of the Theorem 1:

Define m_i is the maximum eigenvalue of b_i, n_i is the minimum eigenvalue of τ_i , the filter error vectors and adaptive estimation error vectors are defined as:

$$\begin{cases} g_1 = x_{2c} - \tilde{x}_{2d} \\ g_2 = x_{3c} - \tilde{x}_{3d} \\ \tilde{e}_i = d_i - \hat{k}_i (i = 1,2,3) \end{cases} \tag{11}$$

Then we have:

$$\begin{aligned} \dot{g}_1 = \dot{x}_{2c} - \dot{\tilde{x}}_{2d} = -T_1^{-1}g_1 - \dot{\tilde{x}}_{2d} \\ \dot{g}_2 = \dot{x}_{3c} - \dot{x}_{3d} = -T_2^{-1}g_2 - \dot{x}_{3d} \end{aligned} \tag{12}$$

For simplification, define $S_1^* = \tilde{x}_2 - x_{2c}$.

Define the candidate Lyapunov function as:

$$V = \frac{1}{2}\sum_1^3 S_i^T S_i + \frac{1}{2}\sum_1^2 g_i^T g_i + \frac{1}{2}\sum_1^3 \frac{e_i^T e_i}{r_i} \tag{13}$$

Take a time derivative to have:

$$\dot{V} = \sum_1^3 S_i^T \dot{S}_i + \sum_1^2 g_i^T \dot{g}_i + \sum_1^3 e_i^T \dot{e}_i \tag{14}$$

then direct computations are as follow:

$$\begin{aligned} & S_1^T \dot{S}_1 + g_1^T \dot{g}_1 + e_1^T \dot{e}_1 \\ & = S_1^T (f_1 + b_1\tilde{x}_2 + cx_1 + d_1) + g_1^T \dot{g}_1 + e_1^T \dot{e}_1 \\ & = S_1^T b_1 (S_1^* + g_1) + S_1^T (-\tau_1 S_1 - P_1\hat{k}_1 + d_1) + g_1^T \dot{g}_1 + e_1^T \dot{e}_1 \\ & \leq \frac{m_1}{2} S_1^T S_1 + \frac{m_1}{4} S_2^T S_2 + \frac{m_1}{4} g_1^T g_1 + g_1^T \dot{g}_1 - e_1^T \dot{\hat{k}}_1 + \\ & S_1^T (-\tau_1 S_1 - P_1\hat{k}_1 + d_1) \\ & \leq \frac{m_1}{4}(2S_1^T S_1 + S_2^T S_2 + g_1^T g_1) - n_1 S_1^T S_1 - S_1^T (P_1\hat{k}_1 - d_1) \\ & -e_1^T \dot{\hat{k}}_1 + g_1^T (-n_1 + \frac{1}{2}\|\dot{\tilde{x}}_{2d}\|^2) + \frac{1}{2} \\ & \leq (-n_1 + \frac{m_1}{2}) S_1^T S_1 + \frac{m_1}{4} S_2^T S_2 + (-n_1 + \frac{m_1}{4} + \frac{1}{2}\|\dot{\tilde{x}}_{2d}\|^2) g_1^T g_1 + \frac{1}{2} \\ & -S_1^T (P_1\hat{k}_1 - d_1) - e_1^T \dot{\hat{k}}_1 \\ & = -\begin{bmatrix} s_{11} \\ s_{12} \end{bmatrix}^T \begin{bmatrix} sign(s_{11})\hat{k}_{11} \\ sign(s_{12})\hat{k}_{12} \end{bmatrix} + \begin{bmatrix} s_{11} \\ s_{12} \end{bmatrix}^T d_1 - r_1(d_1 - \hat{k}_1)^T \begin{bmatrix} |s_{11}| \\ |s_{12}| \end{bmatrix} \\ & \leq -\sum_{i=1}^2 \hat{k}_{1i}|s_{1i}| + \sum_{i=1}^2 k_{1i}|s_{1i}| - r_1\sum_{i=1}^2 |s_{1i}|(k_{1i} - \hat{k}_{1i}) \\ & \leq -(r_1 - 1)\sum_{i=1}^2 k_{1i}|s_{1i}| \end{aligned}$$

Consider that $r_1 \geq 1$, so we have:

$$\begin{aligned} & S_1^T \dot{S}_1 + g_1^T \dot{g}_1 + e_1^T \dot{e}_1 \\ & \leq (-n_1 + \frac{m_1}{2}) S_1^T S_1 + \frac{m_1}{4} S_2^T S_2 + (-n_1 + \frac{m_1}{4} + \frac{1}{2}\|\dot{\tilde{x}}_{2d}\|^2) g_1^T g_1 \\ & -(r_1 - 1)\sum_{i=1}^2 k_{1i}|s_{1i}| + \frac{1}{2} \\ & \leq (-n_1 + \frac{m_1}{2}) S_1^T S_1 + \frac{m_1}{4} S_2^T S_2 + (-n_1 + \frac{m_1}{4} + \frac{1}{2}\|\dot{\tilde{x}}_{2d}\|^2) g_1^T g_1 + \frac{1}{2} \end{aligned}$$

The same reason, we can learn that:

$$S_2^T\dot{S}_2 + g_2^T\dot{g}_2 + e_2^T\dot{e}_2$$
$$\le (-n_2 + \frac{m_2}{2})S_2^T S_2 + \frac{m_1}{4} S_3^T S_3 + (-n_2 + \frac{m_2}{4} + \frac{1}{2}\|\dot{\bar{x}}_{3d}\|^2) g_2^T g_2$$
$$-(r_2 - 1)\sum_{i=1}^{3} k_{2i}|s_{2i}| + \frac{1}{2}$$
$$\le (-n_2 + \frac{m_2}{2})S_2^T S_2 + \frac{m_1}{4} S_3^T S_3 - (n_2 - \frac{m_2}{4} - \frac{1}{2}\|\dot{\bar{x}}_{3d}\|^2) g_2^T g_2 + \frac{1}{2}$$

$$S_3^T\dot{S}_3 + e_3^T\dot{e}_3$$
$$\le -n_3 S_3^T S_3 - (r_3 - 1)\sum_{i=1}^{3} k_{3i}|s_{3i}|$$
$$\le -n_3 S_3^T S_3$$

In summary, we have:

$$\dot{V} = \sum_1^3 S_i^T\dot{S}_i + \sum_1^2 g_i^T\dot{g}_i + \sum_1^3 e_i^T\dot{e}_i$$
$$\le -(n_1 - \frac{m_1}{2})S_1^T S_1 - (n_2 - \frac{m_2}{2} - \frac{m_1}{4})S_2^T S_2 - (n_3 - \frac{m_2}{4})S_3^T S_3$$
$$-(n_1 - \frac{m_1}{4} - \frac{1}{2}\|\dot{\bar{x}}_{2d}\|^2) g_1^T g_1 - (n_2 - \frac{m_2}{4} - \frac{1}{2}\|\dot{\bar{x}}_{3d}\|^2) g_2^T g_2 + 1$$

By some calculations we can learn that $\|\dot{\bar{x}}_{2d}\|^2, \|\dot{\bar{x}}_{3d}\|^2$ are bounded. So when the parameters satisfy the inequality below:

$$\begin{cases} n_1 \ge \frac{m_1}{2} \\ n_2 \ge \frac{m_2}{2} + \frac{m_1}{4} \\ n_3 \ge \frac{m_2}{4} \\ n_1 \ge \frac{m_1}{4} + \frac{1}{2}\|\dot{\bar{x}}_{2d}\|^2 \\ n_2 \ge \frac{m_2}{4} + \frac{1}{2}\|\dot{\bar{x}}_{3d}\|^2 \end{cases} \quad (15)$$

then we have [9]:

$$\dot{V} \le -\nu V + C \quad (16)$$

Therefore, S_1, S_2, S_3, g_1, g_2, e_1, e_2, e_3 are all uniformly ultimately bounded (UUB) stable under the condition (15). Furthermore, the states parameters of the nonlinear system (8) are all UUB stable.

IV. Simulation Results Analysis

In this part, the feasibility and effectiveness of the designed 3D-IGC algorithm with terminal angular constraint is certified by a series of numerical simulations for the nonlinear dynamic IGC model of the homing missile in the 3D space.

Consider the following two types of target maneuvers:

Case 1: $a_{t\theta} = a_{t\phi} = 19.6\cos(t) m/s^2$

Case 2: $a_{t\theta} = a_{t\phi} = 0 m/s^2$

The parameters of the system are shown as:

TABLE I. Parameters Of The Model

Symbol	Value	Symbol	Value	Symbol	Value
S	0.42m^2	m_z^α	-28.16	c_y^α	57.16
L	0.68m	$m_z^{\delta_z}$	-27.92	c_y^β	0.08
m	1200kg	m_y^β	-27.31	$c_y^{\delta_z}$	5.74
ρ	1.1558kg/m^3	$m_y^{\delta_y}$	-26.57	c_z^α	-56.31
J_x	100kg·m^2	m_x^α	0.46	c_z^β	-5.62
J_y	5700kg·m^2	m_x^β	-0.37	$c_z^{\delta_y}$	0.09
J_z	5600kg·m^2	$m_x^{\delta_x}$	2.12		

TABLE II. Initial Engagement Parameters

Symbol	Value	Symbol	Value
θ(0)	45π/180rad	V_m	600m/s
$\Phi_c(0)$	0 rad	V_t	600 m/s
ω_x	0.1 rad/s	$x_t(0)$	11136 m
ω_y	0.1 rad/s	$y_t(0)$	8603 m
ω_z	0.2 rad/s	$z_t(0)$	5192.8 m
$x_m(0)$	0 m	θ_{Lf}	30 deg
$y_m(0)$	0 m	φ_{Lf}	-30 deg
$z_m(0)$	0		

The parameters of the controller (8) are as follows:

$$\tau_{11} = \tau_{12} = 2, \tau_{21} = \tau_{22} = \tau_{23} = 1, \tau_{31} = \tau_{32} = \tau_{33} = 10,$$
$$r_1 = 2, r_2 = r_3 = 1, T_1 = T_2 = 0.1.$$

Fig.2-5 show the numerical simulation results.

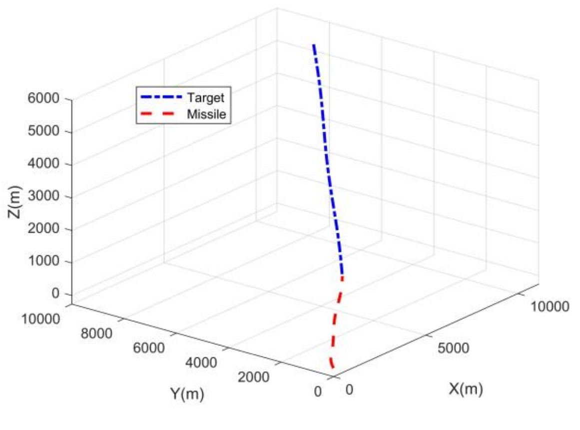

Fig. 2 Movement curves with case 1

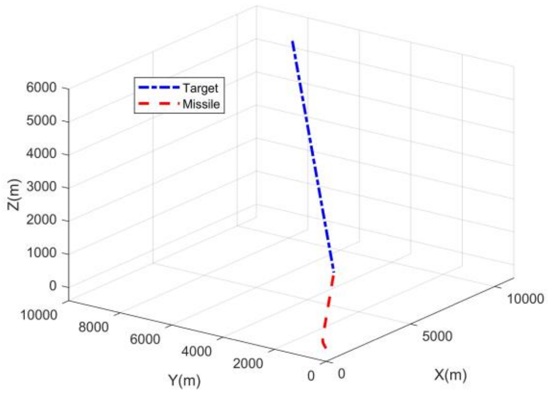

Fig. 3 Movement curves with case 2

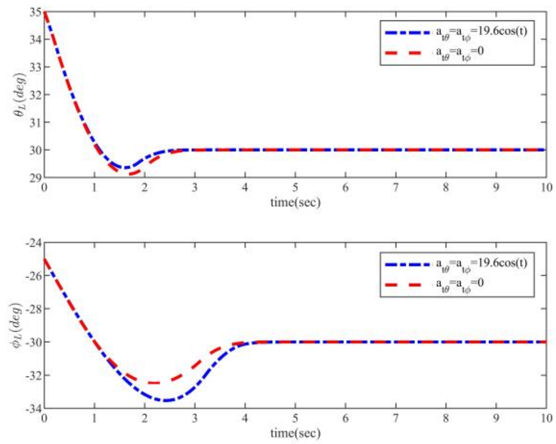

Fig. 4 Curve graph of LOS angle

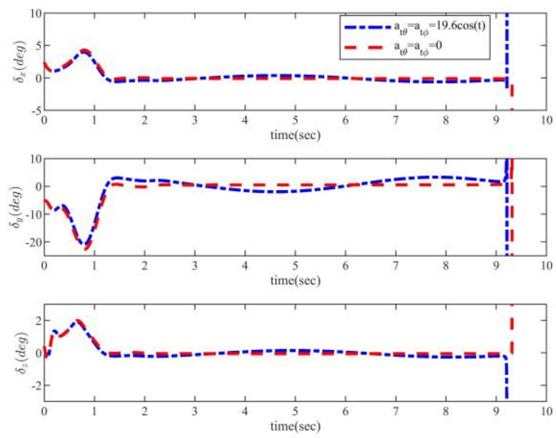

Fig. 5 Curve graph of fin deflections

TABLE III. GUIDANCE PERFORMANCE INDEX

Case	Miss distance(m)	Interception time(s)
Case1	0.271	9.214
Case2	0.175	9.316

From the above table we can learn that the interception time of the two maneuver cases is not much different, and the miss distance is within a reasonable range.

Fig.2 and 3 show that despite the different maneuvering modes of the target, the missile can ultimately intercept the target with a reasonable small miss distance.Fig.4 shows that the terminal impact angles converge to the expected angles, which satisfy the requirement of the terminal angular constraint. Fig.5 shows that the change of the fin deflections is within a reasonable range. These indicates that the design objectives of the IGC system are achieved.

V. CONCLUSION

In this article, a control strategy of 3D-IGC with terminal angular constraint for homing missile is proposed. A time-varying nonlinear IGC model with uncertainties is first established and the adaptive multiple sliding surface control law is devised combined with the backstepping method. The stability of the closed-loop 3D-IGC system is certified via the Lyapunov stability theory. The digital simulation results have validated the achievement of reasonable small miss distance and desired terminal LOS angles simultaneously, which confirms the effectiveness and robustness of the proposed control approach.

REFERENCES

[1] Shijie Fan, and Hongqi Fan. New progress in the design of estimator and guidance law in terminal guidance [J]. Journal of Automatica Sinica, 2015, 41(1):38-46.

[2] Menon PK, and Ohlmeyer EJ. Integrated design of agile missile guidance and autopilot systems [J]. Control Engineering Practice, 2001, 9(2):1095-1106.

[3] Williams D. E., and Richman J.. Design of an integrated strapdown guidance and control system for a tactical missile [C]. AIAA Guidance and Control Conference, 1983:57-66.

[4] Palumbo NF, Reardon BE, and Blauwkamp RA. Integrated guidance and control for homing missiles [C]. Johns Hopkins APL Technical Digest, 2004, 25(2): 121-138.

[5] Shima T, Idan M, and Golan O M.. Sliding Mode Control for Integrated Missile Autopilot-Guidance [J]. Journal of Guidance Control & Dynamics, 2006, 9(2):250-260.

[6] Yan Han. Integrated guidance and control for dual-control missiles based on small-gain theorem [J]. Automatica 2012, 48(10):2686-2692.

[7] E. Lavretsky and N. Hovakimyan, Positive u-modification for stable adaptation in dynamic inversion based adaptive control with input saturation, in Proc. Amer. Control Conf., pp.3373-3378,2005

[8] Sheng Sun, Huaming Zhang, and Di Zhou. The Terminal Angle Constrained Sliding Mode Guidance Law Considering the Dynamic Characteristics of Autopilot [J]. Journal of Astronautics, 2013, 31(1):69-78.

[9] Yan H , Ji H. Integrated guidance and control for dual-control missiles against ground fixed targets [C]. International Conference on Mechatronics & Automation. IEEE, 2012:162-168.